Inorganic Chemistry

Article

pubs.acs.org/IC

Stepwise Formation of a Pentanuclear Ni_4Cu Heterometallic Complex Exhibiting a Vertex-Sharing Defective Double-Cubane Core and Diphenoxo- and Phenoxo/Azide Bridging Groups: A Magnetostructural and DFT Theoretical Study

Koushik Pramanik,[†] Pijush Malpaharia,[†] Antonio J. Mota,[‡] Enrique Colacio,*[,‡] Babulal Das,[§] F. Lloret,[⊥] and Swapan K. Chandra*[,†]

[†]Department of Chemistry, Visva Bharati University, Santiniketan 731 235, India

[‡]Departamento de Química Inorgánica, Facultad de Ciencias, Universidad de Granada, Avenida Fuentenueva s/n, 18002 Granada, Spain

[§]Department of Chemistry, Indian Institute of Technology, Guwahati 781 039, India

[⊥]Instituto de Ciencia Molecular, Universitat de València, 46980 Paterna, València, Spain

Supporting Information

ABSTRACT: Sequential reaction of a N_5O_3 octadentate tripodal ligand with Ni^{2+} and subsequently with Cu^{2+} and azide ligand afforded the first example of a heterobridged (phenoxo/$\mu_{1,1}$-azido) pentanuclear heterometallic (Ni_4Cu) compound, which exhibits a centrosymmetric vertex-sharing defective double-cubane structure. The study of the magnetic properties reveals that the compound shows ferromagnetic interaction interactions, leading to an $S = {}^9/_2$ spin ground state. Density functional theory calculations on the X-ray structure and model compounds predict ferromagnetic interactions through the magnetic exchange pathways involving each couple of metal ions.

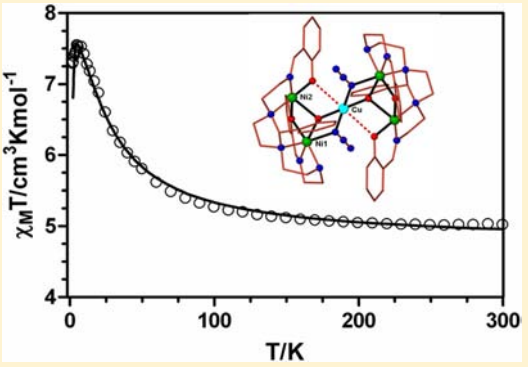

INTRODUCTION

Coordination clusters have attracted much attention during the last three decades not only because of their relevance to bioinorganic chemistry[1] but also because of their potential as new molecule-based magnetic materials.[2] It should be noted that, although a huge number of paramagnetic cluster complexes exhibiting magnetic exchange interactions between metal centers have been reported so far, in only a few are the interactions ferromagnetic (F) in nature. The achievement of F coupling between metal ions is still an interesting challenge for synthetic chemists not only because of its relative scarcity but also because it leads to high-spin ground states, one of the most important requirements for a cluster metal complex to exhibit potential applications as single-molecule magnets (SMMs)[3] and low-temperature magnetic coolers.[4] Although there exist numerous examples of transition-metal homometallic polynuclear complexes containing either azide[5e−g] or phenoxo bridging groups,[5a−d] only few of them are either heterobridged systems,[6] having a combination of both bridging groups, or heterometallic compounds.[7] In view of the above considerations and taking into account that heterometallic complexes, in general, exhibit a richer variety of magnetic properties than homometallic complexes, we decided to use a new octadentate ligand (H_3L; Figure 1) to prepare heterometallic heterobridged

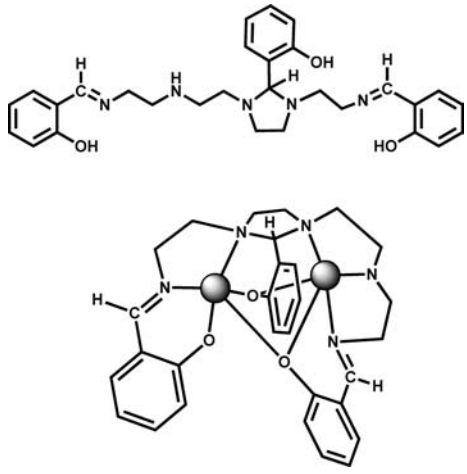

Figure 1. Top: Structure of the H_3L ligand. Bottom: Coordination mode of the ligand giving rise to the Ni_2 metalloligand species.

Received: December 23, 2012
Published: March 11, 2013

   dx.doi.org/10.1021/ic302784q | *Inorg. Chem.* 2013, 52, 3995−4001

clusters containing phenoxo/azido-bridged groups with presumable high-spin ground states. In this paper, we report the synthesis, structural characterization, and magnetic properties of the first example of this kind of system, the pentanuclear complex $[Ni_4Cu(L)_2(N_3)_2](ClO_4)_2\cdot 2(CH_3)_2CO$ (**1**).

EXPERIMENTAL SECTION

General Procedures. All manipulations were performed under aerobic conditions using reagents and solvents as received.

Synthetic Procedures. *Synthesis of Ligand H_3L.* The ligand H_3L was prepared via condensation reactions similar to those previously reported for a similar ligand.[8] Tetraethylenepentamine (3.80 g, 20 mmol) and salicylaldehyde (7.30 g, 60 mmol) were refluxed in 20 mL of dehydrated alcohol for about 8 h and cooled to room temperature. The resulting solution was filtered, and the solvent from the filtrate was removed by rotary evaporation. The brown semisolid mass was then recrystallized from hot ethanol. The product was isolated as a brown waxy material after drying in vacuum over P_4O_{10}. The yield was 8.90 g (~89%). Anal. Calcd for $C_{29}H_{35}N_5O_3$ (H_3L): C, 69.43; H, 6.98; N, 13.95. Found: C, 69.31; H, 6.82; N, 14.03.

Synthesis of $[Ni_4Cu(L)_2(N_3)_2](ClO_4)_2\cdot 2(CH_3)_2CO$ (1). A solution of $Ni(ClO_4)_2\cdot 6H_2O$ (0.250 g, 0.68 mmol) in 4:1 acetone/methanol (10 mL) was added to a solution of H_3L (0.170 g, 0.34 mmol) in 4:1 acetone/methanol (10 mL) over a period of 15 min. A yellow-orange solution was produced that was stirred for 10 min. To this was added slowly with constant stirring an aqueous methanolic solution (1 mL of water + 2 mL of methanol) of NaN_3 (0.022g, 0.34 mmol). To the resulting deep-brown solution was added slowly a solution of $Cu(ClO_4)_2\cdot 6H_2O$ (0.063 g, 0.17 mmol) in 4:1 acetone/methanol (10 mL). The resulting deep-brown solution was then kept for slow evaporation. After 5 days, brown crystals of **1** were obtained (0.180 g, ~67% yield) that were suitable for X-ray crystallography. These were collected by filtration and dried in vacuum to obtain desolvated species. Anal. Calcd for $C_{58}H_{64}N_{16}O_{14}Cl_2Ni_4Cu$ (**1**): C, 44.13; H, 4.09; N, 14.20; Ni, 14.87; Cu, 4.03. Found: C, 44.05; H, 3.98; N, 14.11; Ni, 14.71, Cu, 4.07. IR (cm^{-1}): 2078, 2070, 1646, 1082, 624.

Physical Measurements. Elemental analyses for carbon, hydrogen, and nitrogen were performed using a Perkin-Elmer 2400II elemental analyzer. Nickel contents were determined gravimetrically as the nickel dimethylglyoximate complex. Copper contents were determined iodometrically using standard $Na_2S_2O_3$, which was standardized against a standard $K_2Cr_2O_7$ solution. Magnetization and variable-temperature (2−300 K) magnetic susceptibility measurements on polycrystalline samples were carried out with a Quantum Design SQUID MPMS XL-5 device operating at different magnetic fields. The experimental susceptibilities were corrected for diamagnetism of the constituent atoms using Pascal's tables. IR spectra (as KBr pellets, 4000−400 cm^{-1}) were taken at 298 K using a Shimadzu model 8400 S spectrophotometer. Electrospray ionization mass spectrometry (ESI-MS) spectra were recorded with a Waters QTOF Micro YA263 on a yellow-orange solution containing $Ni(ClO_4)_2\cdot 6H_2O$ (0.250 g, 0.68 mmol) and H_3L (0.170 g, 0.34 mmol) in 4:1 acetone/methanol (10 mL), which was stirred for 10 min. Variable-temperature electron paramagnetic resonance (EPR) measurements in the 300−4 K range were recorded on a Bruker 300 E spectrometer operating at the X band (9.2 GHz).

Crystal Structure Determinations and Refinement of 1. Single crystals suitable for X-ray crystallographic analysis were selected following examination under a microscope. The X-ray diffraction data were collected at 296 K with Mo Kα radiation (λ = 0.71073 Å) using a Bruker Nonius SMART CCD diffractometer equipped with a graphite monochromator. Intensity data were collected in the $\omega-2\theta$ scan mode. The data were corrected for Lorentz, polarization, and absorption effects, the latter using *SADABS*.[9] The structure was solved by direct methods, and the structure solution and refinement were based on $|F|^2$. The non-hydrogen atoms were refined anisotropically. The aliphatic and aromatic hydrogen atoms were calculated and refined using a riding model, whereas the amine hydrogen atoms were localized through difference synthesis. The atomic scattering factors and anomalous dispersion terms were taken from the standard compilation.[10] The structure was solved with *SHELXS97* and refined with *SHELXL97*.[11,12] Crystal data and data collection details are collected in Table S1 in the Supporting Information (SI).

Computational Details. All theoretical calculations were carried out at the density functional theory (DFT) level using the hybrid B3LYP exchange-correlation functional,[13] as implemented in the *Gaussian 09* program.[14] A quadratic convergence method was employed in the self-consistent-field process.[15] The triple-ζ quality basis set proposed by Ahlrichs and co-workers has been used for all atoms.[16] Calculations were performed on complexes built from experimental geometries as well as on model complexes. The electronic configurations used as starting points were created using *Jaguar 7.9* software.[17] The approach used to determine the exchange coupling constants for polynuclear complexes has been described in detail elsewhere.[18]

RESULTS AND DISCUSSION

The octadentate ligand H_3L (Figure 1) was prepared in good yield by condensation of tetraethylene pentamine and salicylaldehyde in a 1:3 molar ratio using ethanol as the solvent. This ligand is based on an imidazolidine framework with one phenol linked to the C1 atom and two different salicylaldimine arms bonded to the N1 and N3 atoms. Reaction of the H_3L ligand (see Figure 1) with $Ni(ClO_4)_2\cdot 6H_2O$ in an acetone/methanol mixture (4:1, v/v) and successively with NaN_3 and $Cu(ClO_4)_2\cdot 6H_2O$ in a 1:2:1:0.5 $H_3L/Ni/N_3/Cu$ molar ratio using methanol as the solvent led to complex **1**.

The ligand is specifically designed to form diphenoxo-bridged dinuclear Ni^{2+} complexes and, therefore, in a first step, $[Ni(\mu\text{-}L)Ni]^+$ species should be generated in solution (Figure 1). In a second step, these Ni_2 metalloligands would react with N_3^- and further with Cu^{2+} through the donor oxygen atoms of the coordinated phenolate groups to afford the Ni_4Cu pentanuclear complex **1**.

The formation of $[(Ni(\mu\text{-}L)Ni]^+$ dinuclear species during the first step of the reaction is evidenced by detection of the molecular ion peak centered at m/z 614 in the ESI-MS^+ spectrum of the solution obtained immediately after mixing of the ligand and $Ni(ClO_4)_2\cdot 6H_2O$ in a 4:1 acetone/methanol mixture (Figure S1 in the SI). When the solution is allowed to stand for 1 week at room temperature, the molecular ion peak is also observed, thus suggesting that the $[(Ni(\mu\text{-}L)Ni]^+$ dinuclear species is rather stable in an acetone/methanol solution.

The structure of **1** is made of centrosymmetric pentanuclear $[Ni_4Cu(L)_2(N_3)_2]^{2+}$ cationic units, two perchlorate anions, and two acetone crystallization molecules, the latter semicoordinated to one of the Ni^{II} ions, which are well isolated in the crystal. A perspective view of the structure of **1** is given in Figure 2, whereas selected bond lengths and angles are gathered in Tables S1 and S2 in the SI, respectively.

Within the pentanuclear $[Ni_4Cu(L)_2(N_3)_2]^{2+}$ unit, each octadentate non-symmetrical tripodal L^{3-} ligand wraps around two Ni^{2+} metal ions in such a way that two oxygen atoms belonging to phenolate groups (those connected to the imidazolidine ring through the shortest and longest arms) bridge these two Ni^{2+} ions. Each of the two diphenoxo-bridged dinuclear units is connected to the central Cu^{2+} atom, which is located at the center of symmetry, through two phenoxo and one end-on azide bridges to form the pentanuclear $[Ni_4Cu(L)_2(N_3)_2]^{2+}$ with a vertex-sharing defective double-cubane core. One of the phenoxo bridging groups (that linked to the carbon atom of the imidazolidine ring) connects simultaneously

dx.doi.org/10.1021/ic302784q | *Inorg. Chem.* 2013, 52, 3995−4001

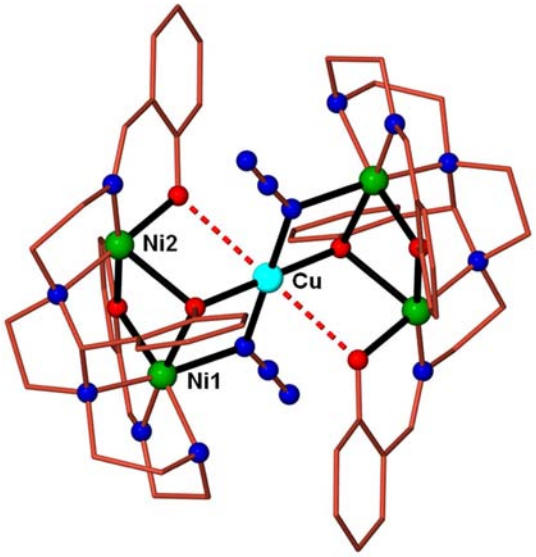

Figure 2. Perspective view of the structure of **1**. Acetone molecules, perchlorate anions, and hydrogen atoms have been omitted for the sake of clarity. Color code: N, blue; O, red; Ni, green; Cu, light blue; C, light brown. Dashed lines represent the semicoordinated Cu–O bonds.

the two Ni^{2+} ions and the Cu^{2+} ion and therefore acts as a μ_3-bridging group. The Ni1 atom exhibits a N_4O_2 octahedral coordination environment, which is made by the coordination of three nitrogen atoms belonging to amino groups of the ligand, one nitrogen atom belonging to the azide bringing group, and two oxygen atoms from the μ_2- and μ_3-phenoxo bridging groups, which are located in cis positions. The Ni–O and Ni–N distances are in the range of 1.978–2.128 Å. The Ni2 ion displays a rather distorted square-pyramidal geometry, in which the three phenoxo oxygen atoms occupy *fac* positions. In the equatorial plane, the Ni–O and Ni–N bond distances are between 1.945 and 2.112 Å, whereas the oxygen atoms belonging to the semicoordinated acetone and to the μ_3-phenoxo group occupy the axial positions at longer distances of 2.671 and 2.303 Å, respectively. The Ni–O–Ni bridging angles in each of the diphenoxo-bridged dinuclear units are 88.28° and 99.78°, and the Ni···Ni distance is 3.063 Å. The Cu^{2+} ion exhibits a tetragonally distorted CuN_2O_4 coordination environment, as expected for the Jahn–Teller effect. Four short bonds of ∼2 Å are formed with the two nitrogen atoms of the azide bridging ligands and the two oxygen atoms of the μ_3-phenoxo bridging groups connecting Ni^{2+} and Cu^{2+} ions, whereas the axial positions are occupied by the oxygen atoms belonging to μ_2-phenoxo bridging groups, which are semicoordinated with a Cu–O bond distance of 2.779 Å. The Cu–N–Ni and Cu–O–Ni angles are 101.80° and 101.69°, respectively. The Cu···Ni distance is 3.172 Å. The $Ni(O)_2Ni$ bridging fragment is folded with a hinge angle of 23.1° (dihedral angle between the O–Ni–O planes), whereas the Cu(NO)Ni and $Cu(O)_2Ni$ bridging fragments are almost planar with hinge angles of 7.5° and 2.0°, respectively. Finally, the carbon atom of the phenolic ring is shifted by ∼137° with respect the $Ni(O)_2Ni$ planes and 119.2° and 153.2° with regard the $Cu(O)_2Ni$ plane.

It should be noted that only a few examples of heterometallic Ni_xCu_y cluster compounds have been reported so far.[19] As far as we now, only one of them is of the Ni_4Cu type, but it exhibitis a square-pyramidal topology of metal ions and *p-tert*-butylthiacalix[6]arene bridging ligands.[20]

The temperature dependence of $\chi_M T$ (χ_M is the molar magnetic susceptibility per Ni_4Cu unit) of **1** in the range 300–2 K is shown in Figure 3.

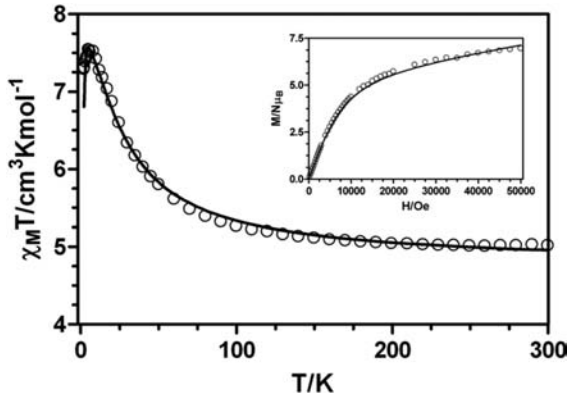

Figure 3. Temperature dependence of $\chi_M T$ for **1**. Inset: Field dependence of magnetization. The solid lines show the best fits with D = 9 cm^{-1} and J_1 = 12.9 cm^{-1} and any of the set of values for J_2 and J_3 indicated in the text. All fits are virtually identical to each other.

The $\chi_M T$ value at room temperature (5.04 cm^3 mol^{-1} K) is higher but close to that expected for four uncoupled Ni^{2+} ions (S = 1) and one Cu^{2+} ion (S = $^1/_2$) with g = 2.0 (4.375 cm^3 mol^{-1} K). The $\chi_M T$ product increases with decreasing temperature, first slightly until ∼100 K and then sharply to reach a maximum value of 7.54 cm^3 mol^{-1} K at 5 K. Below this temperature, the $\chi_M T$ product shows a sharp decrease to reach a value of 7.28 cm^3 mol^{-1} K. The increase before the maximum is in agreement with a dominant F interaction inside the Ni_4Cu units, whereas the decrease of $\chi_M T$ below the maximum is likely associated with the presence of magnetic anisotropy and/or weak antiferromagnetic (AF) interactions between the pentanuclear Ni_4Cu complexes. In connection with this, M versus H/T data (Figure 4) are not superposed on a master curve, thus suggesting the presence of a significant anisotropy and/or low-lying excited states that prevent saturation of magnetization. The presence of low-lying energy levels very close in energy to the ground state would be the reason why all

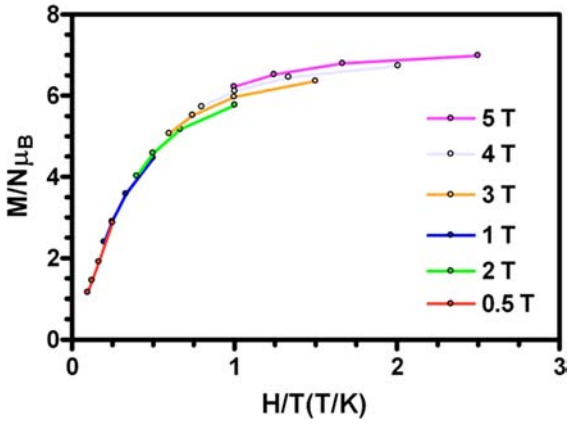

Figure 4. M versus H/T plots for **1** in the range 2–5 K. The solid lines are guides for the eye.

dx.doi.org/10.1021/ic302784q | Inorg. Chem. 2013, 52, 3995–4001

attempts to fit M versus H/T data to extract the magnitude and sign of D in the $S = {}^9/_2$ ground state were unsuccessful.

In keeping with the centrosymmetric structure of **1**, the magnetic susceptibility data were analyzed with the following Hamiltonian (see Scheme 1):

$$H = -J_1(S_{Ni1}S_{Ni2} + S_{Ni3}S_{Ni4}) - J_2(S_{Ni2}S_{Cu} + S_{Cu}S_{Ni4}) - J_3(S_{Ni1}S_{Cu} + S_{Ni3}S_{Cu}) + D_{Ni}\sum_{1}^{4}(S_{zi}^{\,2} - 2/3)$$

Scheme 1. Magnetic Exchange Pathways in Compound 1

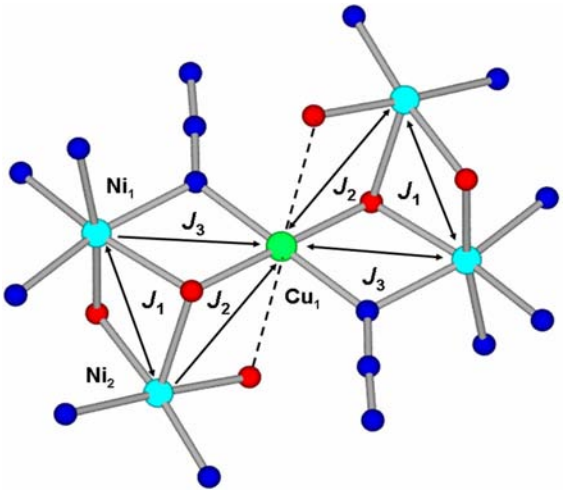

where the first three terms correspond to the isotropic exchange interactions between the Ni^{2+} ions and between the Ni^{2+} and Cu^{2+} ions and the fourth one is the local axial zero-field splitting of the Ni^{2+} ions (all D_{Ni} values were assumed to be equal).

This Hamiltonian was numerically diagonalized by using the *MAGPACK* program.[21] The fitting procedure led to multiple solutions with similar agreement factors depending on the input values of J_1, J_2, and J_3 parameters. In all cases, J_1, g, and D showed values of +12.9 cm^{-1}, 2.08, and 9.0 cm^{-1}, respectively, whereas J_2 and J_3 varied between −3 and +0.5 cm^{-1} and between +7.0 and +3.0 cm^{-1}, respectively. Afterward, D_{Ni} was fixed to zero and a term accounting for the intermolecular interactions by means of the molecular-field approximation, $-zJ'\langle S_z\rangle S_z$, was introduced in the Hamiltonian. Multiple solutions were also obtained, and in all cases, J_1, g, and zJ' exhibited values of +13.4 cm^{-1}, 2.08, and −0.13 cm^{-1}, respectively, and J_2 and J_3 were found in the ranges −2.2 to −0.44 and 7.0−4.2 cm^{-1}, respectively. Moreover, the quality of the fitting did not significantly improve. The D_{Ni} values obtained with $zJ' = 0$ and the zJ' values obtained with $D_{Ni} = 0$ can be considered as the limit values for these parameters because zJ' and D_{Ni} are strongly correlated.

To reduce the number of parameters in the fitting procedure, only the data immediately before the maximum (between 10 and 300 K) were used, thus practically removing the effects of D and/or zJ' on the experimental curve. The fit of these data to the isotropic Hamiltonian led, depending on the input initial values, to J_1 = +13.0 cm^{-1} with J_2 and J_3 varying in the ranges −3.3 to −0.6 and 6.6−1.8 cm^{-1}, respectively. These results are very similar to those using the complete set of experimental data, and the quality of the fit was slightly improved. All fitting procedures show a strong correlation between J_2 and J_3, so that J_3 increases when J_2 decreases and vice versa. It is clear from these results that J_1 can be accurately determined, but there is a great uncertainty in the J_2 and J_3 parameters, which is can be due to overparametrization with this model. In view of this, we decided to fit the data between 10 and 300 K with either J_2 or J_3 fixed to zero, thus obtaining a J_s value for these two parameters together. The best fit led to the following parameters: J_1 = +13.1 cm^{-1}, J_s = +2.4 cm^{-1}, g = 2.08, and $R = 1.4 \times 10^{-6}$. The J_s value is close to the sum of J_2 and J_3 obtained in all of the fitting procedures. It is of interest that the experimental data cannot be fitted using only one J parameter.

It should be noted that either positive or negative values were found for J_2 in the three types of fitting procedures. In order to shed light on the sign of J_2, DFT calculations using the broken-symmetry approach were carried out on the X-ray structures, as found in the solid state.

The calculated J values are given in Scheme 2. As can be seen in this figure, the values for J_1, J_2, and J_3 are all positives. We

Scheme 2. DFT-Calculated J Values for 1

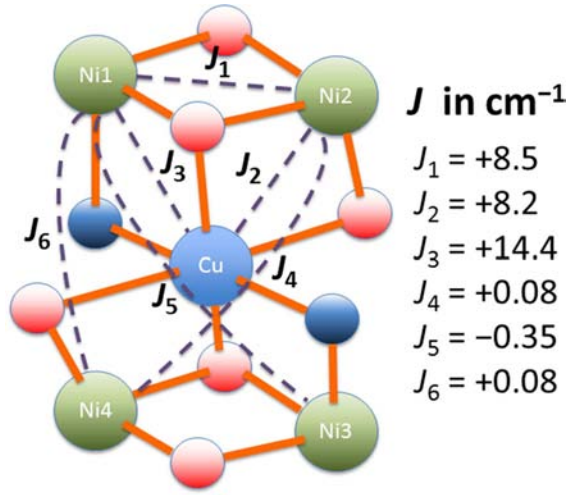

have also performed calculations on two model systems (centrosymmetric pentanuclear Ni_4Cu and trinuclear Ni_2Cu; see Figure S2 in the SI) derived from the X-ray structure by replacing nitrogen coordinated atoms and phenoxo groups by NH_3 and methoxo groups, respectively. For both model compounds, J_1, J_2, and J_3 also are F interactions, thus supporting the sign of these interactions in **1**. It should be remarked that generally these types of DFT calculations correctly predict the sign of the magnetic interactions, but there usually exist discrepancies between the magnitudes of the experimental and calculated J values.[6] This may be due to either the inherent limitations of the method or the flexibility of the structure, which allows some structural changes when the sample is cooled.

Interestingly, as can be seen in Figure 3 and S3 in the SI, the experimental field dependence of magnetization can be well reproduced from any set of J_2 and J_3 values extracted from the fitting of the experimental susceptibility with J_1 = 12.9 cm^{-1}, g = 2.08, and D = +9 cm^{-1}. Because there are two different Ni^{2+} ions in the structure, one exhibiting a distorted square-pyramidal geometry and the other one a distorted octahedral geometry, the D_{Ni} parameter obtained from the fit (+9 cm^{-1}) represents an average value for the two types of Ni^{2+} ions. In

dx.doi.org/10.1021/ic302784q | Inorg. Chem. 2013, 52, 3995−4001

fact, D_{Ni} is intermediate between those usually observed for distorted octahedral Ni^{2+} ions ($D_{Ni} \sim 2-8$ cm^{-1} range)[6] and pentacoordinated Ni^{2+} ions (15−20 cm^{-1} range).[22]

The spin-density distribution for the $^9/_2$ ground state in **1** is shown in Figure 5, whereas the corresponding Mulliken spin-

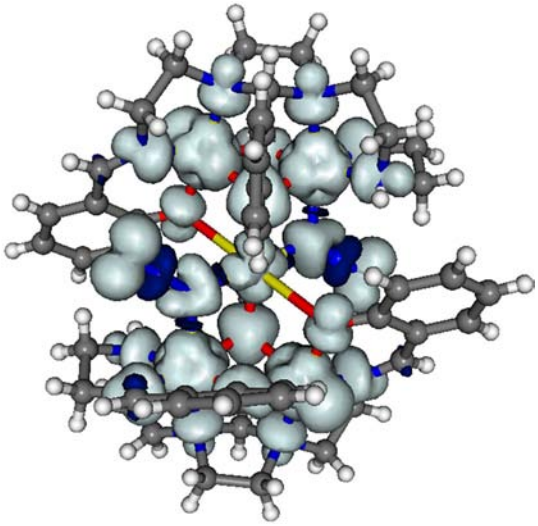

Figure 5. Calculated spin densities for **1**. The isodensity surfaces represented correspond to a cutoff value of 0.0015 e $bohr^{-3}$. Gray and blue colors correspond to positive and negative values, respectively.

density values are given in Table S3 in the SI. As expected for the Ni^{2+} atom, with magnetic orbitals of the $d_{x^2-y^2}$ and d_{z^2} type, the shape of the spin density is octahedral, whereas for the copper(II) atom, the shape of the spin density corresponds to that expected for a $d_{x^2-y^2}$ magnetic orbital. The spin densities on the Ni^{2+} and Cu^{2+} atoms, as well as on the oxygen and nitrogen bridging atoms, clearly show the predominance of the delocalization mechanism through σ-type exchange pathways involving the magnetic orbitals of the Ni^{2+} and Cu^{2+} atoms and the p orbitals of the phenoxo and azide bridging groups. The azido nitrogen atom has a relatively smaller spin density than the phenoxo oxygen atoms, which is likely due to polarization within the N_3^- unit, which is evidenced by the fact that the sign of the spin density alternates along the bridging azido group. The phenoxo oxygen atoms connecting the Ni^{2+} ions have the bigger spin density, which is in agreement with the relatively stronger magnetic exchange interaction observed for this magnetic pathway.

Magnetostructural correlations for a series of centrosymmetric octahedral and square-pyramidal diphenoxo-bridged dinuclear nickel(II) complexes have shown that there exists a linear relationship between the J values and the Ni−O−Ni bridge angle (θ), so that the AF coupling increases when θ increases and the crossover point between F and AF coupling is found at ∼97°.[23] Moreover, in nickel tetramers, magnetostructural correlations predict F coupling for μ_3-OR bridges with Ni−O−Ni angles smaller than ∼99°.[24] Previous DFT calculations carried out on dihydroxo- and dialkoxo-bridged $Ni-O_2-Ni$ dinuclear model complexes[5d] indicated that the τ angle (out-of-plane displacement of the atom linked to the bridging oxygen atom from the Ni_2O_2 plane) is of as much importance as the Ni−O−Ni angle (θ). The calculations predicted AF interactions for τ values in the range 0−30° regardless of the θ angle. Moreover, the magnitude of the AF coupling increases when θ increases for angles bigger than 90°. On the other hand, when the τ angle increases, the AF contributions diminish and an overall F interaction can be observed. The change from AF to F occurs for θ values smaller than 96.5° and τ angles in the 30−60° range. Therefore, the AF coupling is favored when θ increases and τ diminishes. In view of this, it is reasonable to assume that small θ angles (in the vicinity of 90−95°) combined with larger τ values (>30−40°) should lead to F interactions. Complex **1** has average θ and τ values of 94.03° and 43.7° in the $Ni-(O_2)-Ni$ bridging fragment, and therefore the observed F interaction through this pathway (J_1) is not unexpected. In fact, the J_1 value agrees well with those observed for μ-$(OR)_3$ bridges in Ni_4 cubane complexes (compound **1** exhibits a vertex-sharing defective dicubane structure) with Ni−O−Ni angles of ∼97°.[24]

As for the J_2 pathway, the Ni−Cu interaction mediated by μ-$O_{phenoxo}$ is expected to be almost inoperative as $O_{phenoxo}$ is bonded in the axial position of the Cu^{II} atom (dashed line in Scheme 1), where the spin density of the unpaired electron is, if any, negligible (the magnetic orbital $d_{x^2-y^2}$ lies in the plane of the μ_3-$O_{phenoxo}$ and azide nitrogen atoms). Moreover, because of the Jahn−Teller distortion, the Cu−$O_{phenoxo}$ distance is too long for effective spin delocalization. Therefore, the magnetic exchange interaction is mainly mediated by the μ_3-$O_{phenoxo}$ bridge. As far as we know, no examples of single-phenoxo-bridged copper(II)−nickel(II) complexes have been reported so far. However, if we assume that the magnetostructural correlation established for diphenoxodicopper(II) complexes is also operative for single-bridged phenoxodicopper(II) complexes (the few reported examples of these kinds of complexes support this assumption[25]) and single-bridged phenoxonickel(II)copper(II) complexes, a weak exchange interaction (either F or AF) would be expected for the bridging angle observed in **1** (102.21°) because it is close to the crossover point of 99° between F and AF interactions in Ni_4 cubanes with μ_3-$O_{phenoxo}$ bridges.[24] In view of the above considerations and the experimental and calculated J values, it is reasonable to assume that J_2 magnetic pathway can transmit a very weak F interaction.

The third pathway (J_3) consists of two different bridges (μ_3-$O_{phenoxo}$ and $\mu_{1,1}$-azide), and therefore the bridging angles for both exchange pathways should be taken into consideration. As indicated above, if the Ni−$O_{phenoxo}$−Ni bridge angle is greater than 97°, diphenoxo-bridged dinickel(II) complexes exhibit AF interactions and a similar magnetostructural correlation applies for diphenoxo-bridged dicopper(II) complexes.[5a] Theoretical studies on bis($\mu_{1,1}$-azide)dinickel(II)[5a] and bis($\mu_{1,1}$-azide)-dicopper(II)[5a] complexes predicted for the former F exchange interactions with a maximum value at $\theta \sim 104°$, whereas for the latter, the interaction should be F for $\theta < 104°$. Numerous experimental results support the above predictions. It should be noted that there exists only one reported example of a bis($\mu_{1,1}$-azide)nickel(II)−copper(II) heterometallic complex[7a] with θ = 103° and exhibiting F interaction between the Ni^{2+} and Cu^{2+} metal ions. Therefore, it seems that the above magnetostructural correlations for bis($\mu_{1,1}$-azide) homometallic complexes also apply for Cu−Ni heterometallic complexes. In addition to this, the few examples of heterobridged μ-phenoxo-$\mu_{1,1}$-azidodinickel(II) complexes so far reported[6] have been shown to exhibit F interactions with J values in the range 2.85−25.6 cm^{-1} for Ni−O−Ni and Ni−N−Ni angles as high as 107° and 98°, respectively. DFT calculations[6] supported these results because they predicted F interactions, with their magnitude

dx.doi.org/10.1021/ic302784q | Inorg. Chem. 2013, 52, 3995−4001

depending on the Ni−O−Ni/Ni−O and Ni−N−Ni/Ni−N ratios as well as on the asymmetry of the Ni−N distances in the Ni−N−Ni bridging region. In line with this, there is experimental evidence indicating F coupling between the Ni^{2+} ions through double μ_3-OH/end-on azido bridges.[26] If we assume that this behavior also applies for heterometallic copper−nickel complexes, as was indicated elsewhere for bis($\mu_{1,1}$-azide)metal complexes, an F exchange interaction through the J_3 pathway is expected, which matches well with the experimental and theoretical results. The relatively large asymmetry of the Ni−O and Ni−N bond distances in the bridging region of the magnetic exchange pathway described by J_3 could justify the weaker F coupling experimentally found for J_3 compared to that found for J_1.

In light of the considerations above, it is reasonable to conclude that in **1** J_1 is ∼13 cm^{-1}, whereas J_2 and J_3 should be close to ∼0.5 and ∼3 cm^{-1}, respectively

Finally, dynamic alternating-current magnetic susceptibility measurements as a function of the temperature at different frequencies reveal that **1** does not exhibit slow relaxation of magnetization, and therefore SMM behavior, even in the presence of a small external direct-current field of 1000 G to fully or partly suppress the possible quantum-tunneling relaxation of magnetization. This behavior can be due to a positive value of the axial anisotropy of the $S = {}^9/_2$ ground state and/or the fast relaxation through the close low-lying excited states.

In conclusion, we have successfully synthesized for the first time a heterobridged (phenoxo/$\mu_{1,1}$-azido) pentanuclear heterometallic (Ni_4Cu) compound, with a centrosymmetric vertex-sharing defective double-cubane core, from the stepwise reaction of a deliberately designed octadentate tripodal ligand (H_3L) with Ni^{2+} and subsequently with Cu^{2+} and azide ligand. This latter was judiciously chosen because of its ability to bridge metal ions with different coordination modes, some of them transmitting F interactions. The compound exhibits F interactions leading to an $S = {}^9/_2$ spin ground state, but it does not show SMM behavior above 2 K. We are currently exploring the possibility of synthesizing different heterometallic heterobridged pentametallic species by using different metal ions, bridging anions, and also numerous substituted derivatives of the octadentate ligand (H_3L), which could eventually show SMM behavior.

■ ASSOCIATED CONTENT

Ⓢ Supporting Information

X-ray crystallographic file in CIF format for complex **1**, experimental details, and pertinent crystallographic data including data collection, refinement, and selected bond lengths and angles. This material is available free of charge via the Internet at http://pubs.acs.org.

■ AUTHOR INFORMATION

Corresponding Author

*E-mail: ecolacio@ugr.es (E.C.), dr_swapan@sify.com (S.K.C.).

Notes

The authors declare no competing financial interest.

■ ACKNOWLEDGMENTS

This work was supported by grants from the Council of Scientific and Industrial Research and the Department of Science and Technology, New Delhi, Government of India (S.K.C.). E.C. and A.J.M., thank the Ministerio de Educación, Cultura y Deporte (Spain) (Grant CTQ2011-24478), and the Universidad de Granada for financial support. We thank the Centro de Supercomputación de la Universidad de Granada for computational resources. F.L. thanks the MICINN (Spain) (Project CTQ2010-15364), the University of Valencia (Project UV-INVAE11- 38904), and the Generalitat Valenciana (Spain) (Projects PROMETEO/2009/108, GV/2012/051, and ISIC/2012/002) for financial support. We are also grateful to the Visva-Bharati University and DST-FIST program of our department for providing the necessary infrastructural facility. We thank Dr. T.K. Paine, IACS, Kolkota, India, for his contribution to recording ESI-M^+ and EPR spectra.

■ REFERENCES

(1) (a) Kraatz, H. B., Metzler-Nolte, N., Eds. *Concepts and Models in Bioinorganic Chemistry*; Wiley-VCH: Weinheim, Germany, 2006. (b) Bertini, I.; Gray, H. B.; Stiefeld, E. I.; Valentine, J. S.*Biological Inorganic Chemistry: Structure and Reactivity*; University Science Books: Herndon, VA, 2007.

(2) Miller, J. S., Drillon, M., Eds. *Magnetism: Molecules to. Materials*; Wiley-VCH: Weinheim, Germany, 2001−2004; Vols. *I*−*V*.

(3) For some reviews, see: (a) Gatteschi, D.; Sessoli, R. *Angew. Chem., Int. Ed.* **2003**, *42*, 268. (b) Gatteschi, D.; Sessoli, R.; Villain, J. *Molecular Nanomagnets*; Oxford University Press: Oxford, U.K., 2006. (c) Aromí, G.; Brechin, E. K. *Struct. Bonding (Berlin)* **2006**, *122*, 1. (d) Milios, C. J.; Piligkos, S.; Brechin, E. K. *Dalton Trans.* **2008**, 1809. (e) Bagai, R.; Christou, G.. *Chem. Soc. Rev.* **2009**, *38*, 1011.

(4) Evangelisti, M.; Brechin, E. K. *Dalton Trans.* **2010**, *39*, 4672.

(5) (a) Ruiz, E.; Alvarez, S.; Rodríguez-Fortea, A.; Alemany, P.; Pouillon, Y.; Massobrio, C. *Magnetism: Molecules to Materials*; Wiley-VCH: Weinheim, Germany, 2001; Vol. *II*. (b) Venegas-Yazigi, D.; Aravena, D.; Spodine, E.; Ruiz, E.; Alvarez, S. *Coord. Chem. Rev.* **2010**, *254*, 2086. (c) Seppala, P.; Colacio, E.; Mota, A. J.; Sillanpaa, R. *Dalton Trans.* **2012**, *41*, 2648. (d) Palacios, M. A.; Mota, A. J.; Perea-Buceta, J. E.; White, F. J.; Brechin, E. K.; Colacio, E. *Inorg. Chem.* **2010**, *49*, 10156. (e) Stamatatos, Th. C.; Christou, G. *Inorg. Chem.* **2009**, *48*, 3308 (Forum Article). (f) Escuer, A.; Aromi, G. *Eur. J. Inorg. Chem.* **2006**, 4721. (g) Ribas, J.; Escuer, A.; Monfort, M.; Vicente, R.; Cortes, R.; Lezama, L.; Rojo, T. *Coord. Chem. Rev.* **1999**, *193*, 1027.

(6) Sasmal, S.; Hazra, S.; Kundu, P.; Dutta, S.; Rajaraman, G..; Carolina Sañudo, E.; Mohanta, S. *Inorg. Chem.* **2011**, *50*, 7257 and references cited therein.

(7) (a) Suárez-Varela, J.; Maimoun, I. B.; Colacio, E. *Dalton Trans.* **2004**, 3938. (b) Colacio, E.; Costes, J.-P.; Domíguez-Vera, J. M.; Ben Maimoun, I.; Suárez-Varela, J. *Chem. Commun.* **2005**, 534−536. (c) Zhao, J.-P.; Hu, B.-W.; Zhang, X.-F.; Yang, Q.; El Fallah, M. S.; Ribas, J.; Bu, X.-H. *Inorg. Chem.* **2010**, *49*, 11325. (d) Chakraborty, A.; Kumar Ghosh, B.; Ribas-Ariño, J.; Ribas, J.; Maji, T. K. *Inorg. Chem.* **2012**, *51*, 6440.

(8) Karmakar, T. K.; Ghosh, B. K.; Usman, A.; Fun, H.-K.; Rivière, E.; Mallah, T.; Aromí, G.; Chandra, S. K. *Inorg. Chem.* **2005**, *44*, 2391.

(9) Sheldrick, G. M. *SADABS*; University of Göttingen: Göttingen, Germany, 2002.

(10) *International Tables for Crystallography*; Kluwer Academic Publishers: Dordrecht, The Netherlands, 1992.

(11) Sheldrick, G. M. *SHELXS97*; University of Göttingen: Göttingen, Germany, 1997.

(12) Sheldrick, G. M. *SHELXL97*; University of Göttingen: Göttingen, Germany, 1997.

(13) (a) Becke, A. D. *Phys. Rev. A* **1988**, *38*, 3098. (b) Lee, C. T.; Yang, W. T.; Parr, R. G. *Phys. Rev. B* **1988**, *37*, 785. (c) Becke, A. D. *J. Chem. Phys.* **1993**, *98*, 5648.

(14) Frisch, M. J.; Trucks, G. W.; Schlegel, H. B.; Scuseria, G. E.; Robb, M. A.; Cheeseman, J. R.; Montgomery, J. A., Jr.; Vreven, T.; Kudin, K. N.; Burant, J. C.; Millam, J. M.; Iyengar, S. S.; Tomasi, J.;

Barone, V.; Mennucci, B.; Cossi, M.; Scalmani, G.; Rega, N.; Petersson, G. A.; Nakatsuji, H.; Hada, M.; Ehara, M.; Toyota, K.; Fukuda, R.; Hasegawa, J.; Ishida, M.; Nakajima, T.; Honda, Y.; Kitao, O.; Nakai, H.; Klene, M.; Li, X.; Knox, J. E.; Hratchian, H. P.; Cross, J. B.; Adamo, C.; Jaramillo, J.; Gomperts, R.; Stratmann, R. E.; Yazyev, O.; Austin, A. J.; Cammi, R.; Pomelli, C.; Ochterski, J. W.; Ayala, P. Y.; Morokuma, K.; Voth, G. A.; Salvador, P.; Dannenberg, J. J.; Zakrzewski, V. G.; Dapprich, S.; Daniels, A. D.; Strain, M. C.; Farkas, O.; Malick, D. K.; Rabuck, A. D.; Raghavachari, R.; Foresman, J. B.; Ortiz, J. V.; Cui, Q.; Baboul, A. G.; Clifford, S.; Cioslowski, J.; Stefanov, B. B.; Liu, G.; Liashenko, A.; Piskorz, P.; Komaromi, I.; Martin, R. L.; Fox, D. J.; Keith, T.; Al-Laham, M. A.; Peng, C. Y.; Nanayakkara, A.; Challacombe, M.; Gill, P. M. W.; Johnson, B.; Chen, W.; Wong, M. W.; Gonzalez, C.; Pople, J. A. *Gaussian 03*, revision C.02; Gaussian, Inc.: Wallingford, CT, 2004.

(15) Bacskay, G. B. *Chem. Phys.* **1981**, *61*, 385.

(16) Schäfer, A.; Huber, C.; Ahlrichs, R. *J. Chem. Phys.* **1994**, *100*, 5829.

(17) *Jaguar 7.6*; Schrödinger, Inc.: Portland, OR, 2009.

(18) (a) Ruiz, E.; Cano, J.; Alvarez, S.; Alemany, P. *J. Comput. Chem.* **1999**, *20*, 1391. (b) Ruiz, E.; Alvarez, S.; Rodríguez-Fortea, A.; Alemany, P.; Puoillon, Y.; Massobrio, C. In *Magnetism: Molecules to Materials*; Miller, J. S., Drillon, M., Eds.; Wiley-VCH: Weinheim, Germany, 2001; Vol. *II*, p 5572. (c) Ruiz, E.; Rodríguez-Fortea, A.; Cano, J.; Alvarez, S.; Alemany, P. *J. Comput. Chem.* **2003**, *24*, 982. (d) Ruiz, E.; Alvarez, S.; Cano, J.; Polo, V. *J. Chem. Phys.* **2005**, *123*, 164110.

(19) Černák, J.; Kočanová, I.; Orendáč, M. *Comments Inorg. Chem.* **2012**, *33*, 2.

(20) Kajiwara, T.; Shinagawa, R.; Ito, T.; Kon, N.; Iki, N.; Miyano, S. *Bull. Soc. Chem. Jpn.* **2003**, *76*, 2267.

(21) *MAGPACK* program: Borrás-Almenar, J. J.; Clemente-Juan, J. M.; Coronado, E.; Tsukerbalt, B. S. *J. Comput. Chem.* **2001**, *22*, 985.

(22) For example, see: (a) Rebilly, J. N.; Charron, G.; Rivière, E.; Guillot, R.; Barra, A. L.; Duran Serrano, M.; van Slageren, J.; Mallah, T. *Chem.—Eur. J.* **2008**, *14*, 1169−1177. (b) Costes, J. P.; Yamaguchi, T.; Kojima, M.; Vendier, L. *Inorg. Chem.* **2009**, *48*, 5555−5561. (c) Costes, J. P.; Maurice, R.; Vendier, L. *Chem.—Eur. J.* **2012**, *18*, 4031.

(23) Nanda, K. K.; Das, R.; Thompson, L. K.; Venkatsubramanian, K.; Nag, K. *Inorg. Chem.* **1994**, *33*, 1188−1193. Nanda, K. K.; Thompson, L. K.; Bridson, J. N.; Nag, K. *Chem. Commun.* **1994**, 1337−1338.

(24) (a) Halcrow, M. A.; Sun, J. S.; Huffman, J. C.; Christou, G. *Inorg. Chem.* **1995**, *34*, 4167. (b) Clemente-Juan, J. M.; Coronado, E.; Galán-Mascarós, J. R.; Gómez-García, C. J. *Inorg. Chem.* **1999**, *38*, 55. (c) Clemente-Juan, J. M.; Chansou, B.; Donnadieu, B.; Tuchages, J. P. *Inorg. Chem.* **2000**, *39*, 5515. (d) Moragues-Cánovas, M.; Helliwell, M.; Ricard, L.; Rivière, E.; Wernsdorfer, W.; Brechin, E.; Mallah, T. *Eur. J. Inorg. Chem.* **2004**, 2219. (e) Ferguson, A.; Lawrence, J.; Parkin, A.; Sánchez-Benítez, J.; Kamenev, K. V.; Brechin, E. K.; Wernsdorfer, W.; Hill, S.; Murrie, M. *Dalton Trans.* **2008**, 6409.

(25) Choudhury, C. R.; Dey, S. K.; Karmakar, R.; Wu, C.-D.; Lu, C.-Z.; El Fallah, M. S.; Mitra, S. *New J. Chem.* **2003**, *27*, 1360.

(26) Esteban, J.; Alcázar, L.; Torres-Molina, M.; Monfort, M.; Font-Bardia, M.; Escuer, A. *Inorg. Chem.* **2012**, *51*, 5503.